BIOLOGY LETTERS

rsbl.royalsocietypublishing.org

Research

Cite this article: Kahru M, Lee Z, Mitchell BG, Nevison CD. 2016 Effects of sea ice cover on satellite-detected primary production in the Arctic Ocean. *Biol. Lett.* **12**: 20160223. http://dx.doi.org/10.1098/rsbl.2016.0223

Received: 20 March 2016
Accepted: 31 October 2016

Subject Areas:
environmental science, ecology

Keywords:
ocean colour, primary production, global change, sea ice

Author for correspondence:
Mati Kahru
e-mail: mkahru@ucsd.edu

One contribution to the special feature 'Effects of sea ice on Arctic biota'.

Electronic supplementary material is available online at https://dx.doi.org/10.6084/m9.figshare.c.3573246.

THE ROYAL SOCIETY PUBLISHING

Global change biology

Effects of sea ice cover on satellite-detected primary production in the Arctic Ocean

Mati Kahru[1], Zhongping Lee[2], B. Greg Mitchell[1] and Cynthia D. Nevison[3]

[1]Scripps Institution of Oceanography, University of California, San Diego, La Jolla, CA 92093, USA
[2]School for the Environment, University of Massachusetts Boston, Boston, MA 02125, USA
[3]University of Colorado, Boulder, CO 80309, USA

MK, 0000-0002-1521-0356

The influence of decreasing Arctic sea ice on net primary production (NPP) in the Arctic Ocean has been considered in multiple publications but is not well constrained owing to the potentially large errors in satellite algorithms. In particular, the Arctic Ocean is rich in coloured dissolved organic matter (CDOM) that interferes in the detection of chlorophyll *a* concentration of the standard algorithm, which is the primary input to NPP models. We used the quasi-analytic algorithm (Lee *et al*. 2002 *Appl. Opti.* **41**, 5755–5772. (doi:10.1364/AO.41.005755)) that separates absorption by phytoplankton from absorption by CDOM and detrital matter. We merged satellite data from multiple satellite sensors and created a 19 year time series (1997–2015) of NPP. During this period, both the estimated annual total and the summer monthly maximum pan-Arctic NPP increased by about 47%. Positive monthly anomalies in NPP are highly correlated with positive anomalies in open water area during the summer months. Following the earlier ice retreat, the start of the high-productivity season has become earlier, e.g. at a mean rate of -3.0 d yr^{-1} in the northern Barents Sea, and the length of the high-productivity period has increased from 15 days in 1998 to 62 days in 2015. While in some areas, the termination of the productive season has been extended, owing to delayed ice formation, the termination has also become earlier in other areas, likely owing to limited nutrients.

1. Background

Decrease in the summer extent of Arctic sea ice is well known and has been correlated with the apparent increase in net primary production (NPP) in the Arctic Ocean [1–3]. However, many parts of the Arctic Ocean, particularly the shelf areas, are rich in coloured dissolved organic matter (CDOM) [4], which is interfering with the remote detection of chlorophyll *a* (Chla, mg m^{-3}), the primary input to most NPP models. Estimates of NPP using standard satellite Chla are therefore to be treated with caution. In addition to the changes in the magnitude of NPP, the seasonal timing of NPP and other biological processes may also be changing [5] and may have consequences for the Arctic food webs.

2. Methods

We applied the quasi-analytic algorithm [6,7] to daily binned level-3 spectral remote sensing reflectance at approximately 9 km spatial resolution of multiple ocean colour sensors (OCTS, 1996–1997, version 2014.0; SeaWiFS, 1997–2010, version 2014.0; MERIS, 2002–2012, ESA second processing; MODISA, 2002–2016, version 2014.0). The daily time series is incomplete for years 1997 and 2016, which are therefore excluded from annual calculations. The spectral absorption and backscattering coefficients derived with the quasi-analytic algorithm (QAA) at 440 and 490 nm

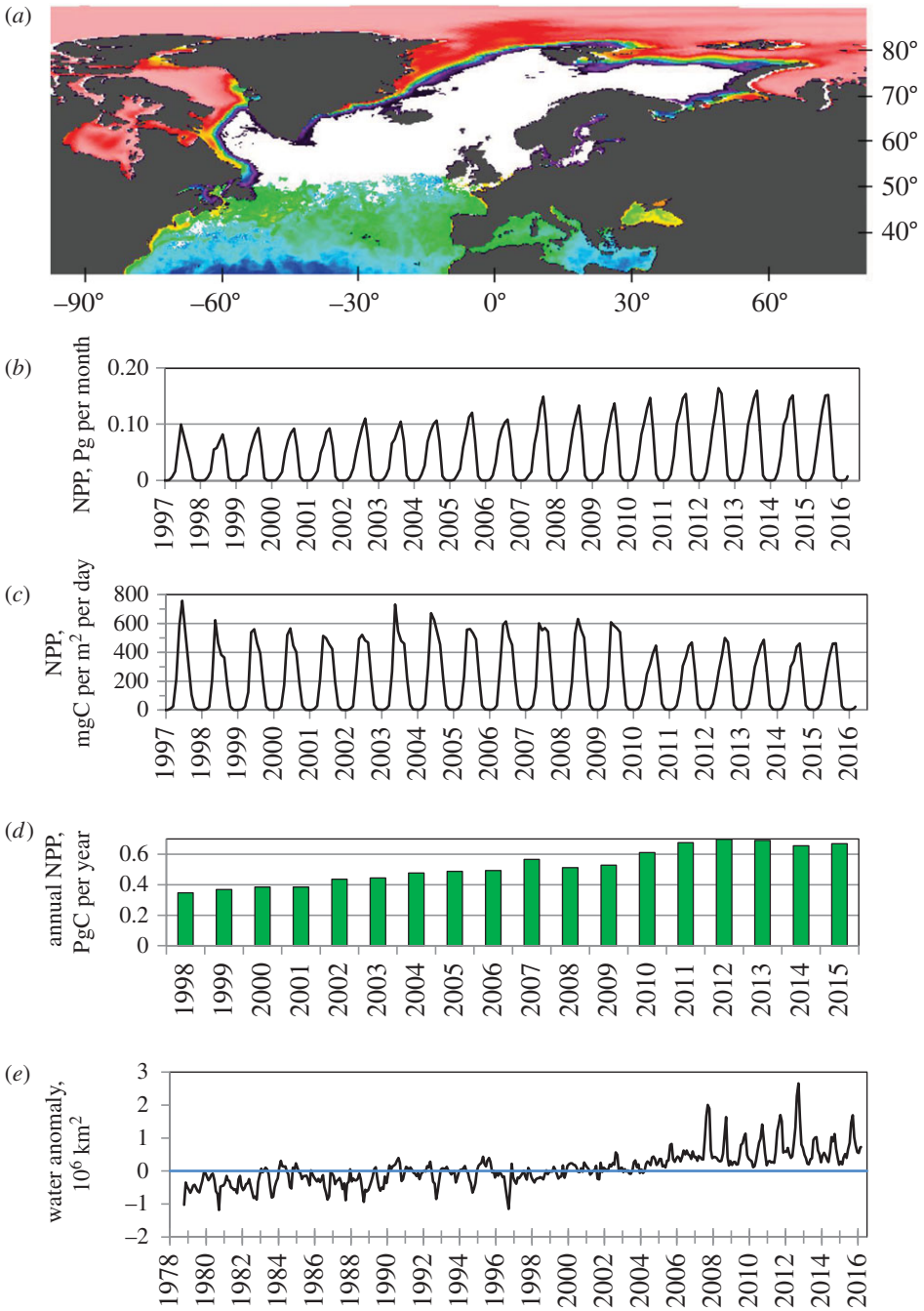

Figure 1. (*a*) Missing ocean colour data during the winter season (January 2015) shown in white, ice cover (pink to purple) in the north and the detected chlorophyll *a* (blue to yellow) in the south. Monthly time series of NPP (*b*) and daily NPP per open water area (*c*) between latitudes 66° N and 84° N. (*d*) Annual pan-Arctic NPP. (*e*) Monthly anomaly of open water area in the Arctic Ocean (between 66° N and 84° N).

wavelengths were merged from different sensors and composited over 5 day periods. Polar oceans are notorious for their cloudiness, which prevents the remote detection of in-water bio-optical variables. While solar radiation can change drastically from day to day and affect NPP, in-water components are temporally less variable and were assumed to be constant during each 5 day period. Daily estimates of NPP were created from daily solar radiance and 5 day composites of in-water bio-optical properties. The vertically generalized production model (VGPM [8]) is a well-known model that ranks among the best in model-to-model comparisons [2,9,10]. We applied the VGPM to the Arctic Ocean with Chla derived from phytoplankton absorption at 440 nm [11], merged photosynthetically active radiation (PAR [12]), the depth of the euphotic zone calculated from the total absorption and backscattering coefficients at 490 nm [13] and using daily optimally interpolated sea surface temperature [14]. PAR was derived by merging estimates from all ocean colour sensors, and filling remaining gaps using an empirical relationship between PAR and surface incoming shortwave irradiance from geostationary and polar orbiting satellites [15]. Daily NPP estimates were composited into 5 day periods by averaging valid data during each 5 day period on a grid of 0.25°. Temporal interpolation between composites was used to fill missing pixels. Spatial interpolation was used to fill remaining missing neighbouring pixel values if the corresponding ice concentration [16] was below 15% using daily sea ice fraction. Sea ice coverage was obtained from NASA Team algorithm datasets (v. 1.1, http://nsidc.org/data/nsidc-0051.html) derived from passive microwave data. More details are provided in the electronic supplementary material. Global 5 day datasets of oceanic NPP are available [17].

In the processing of ocean colour data, pixels with solar zenith angle more than 70° (and sensor zenith angle more than 60°) are excluded. During the winter season, this creates large areas with no ocean colour data (figure 1*a*). While we can

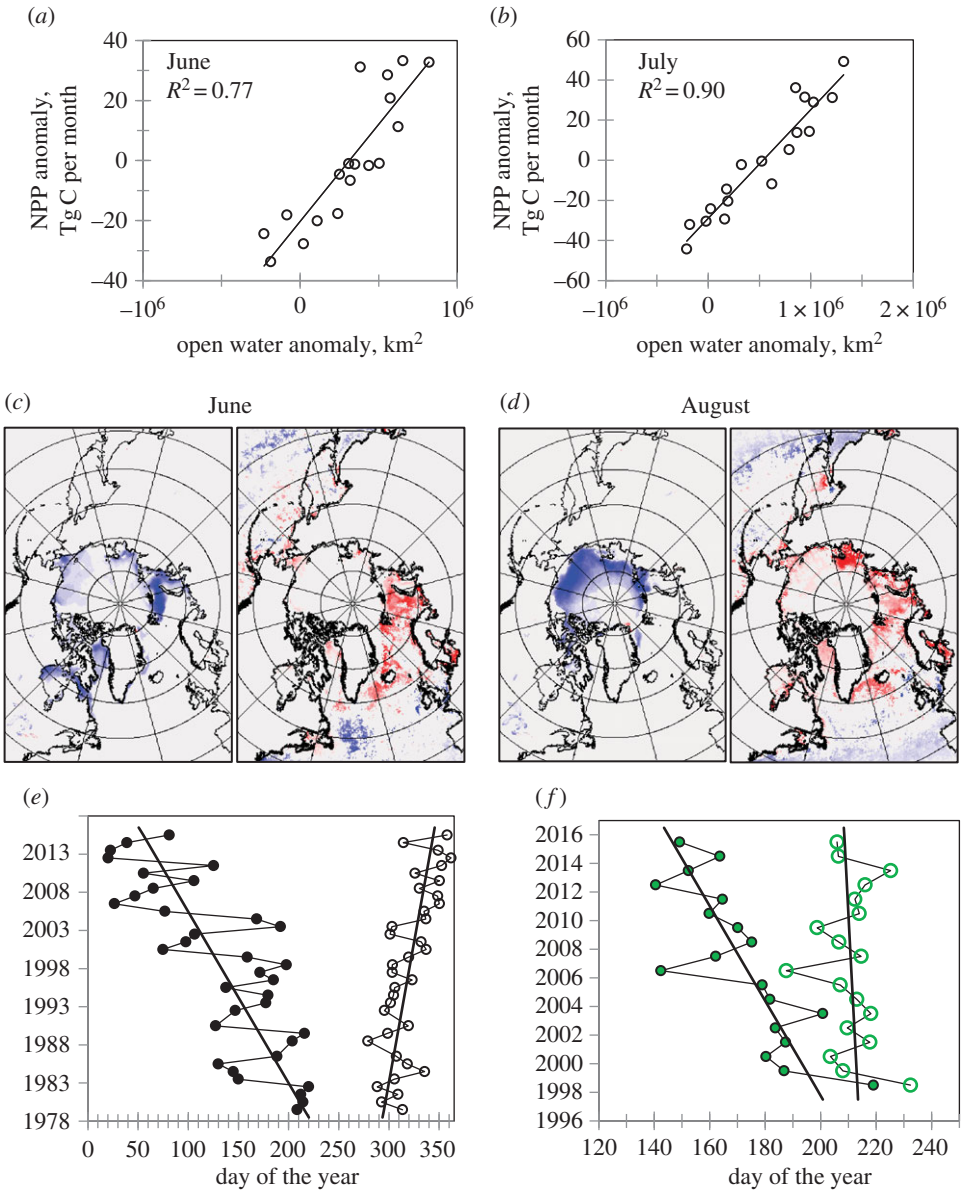

Figure 2. Relationships between anomalies of open water area and pan-Arctic NPP between latitudes 66° N and 84° N in June (*a*) and July (*b*). Spatial trends in interannual changes in ice concentration (left panel) and in NPP (right panel) for the months of June (*c*) and August (*d*). Blue means decrease and red means increase (both at 95% significance). The trends are calculated for the periods of, respectively, 1979–2015 for ice concentration and 1998–2015 for NPP. (*e*) Changes in the timing of the start (filled circles, mean slope -4.5 d yr^{-1}) and end (open circles, mean slope $+1.4$ d yr^{-1}) of the open water period (ice fraction less than 0.15) in northern Barents Sea. (*f*) Changes in the start (filled circles, mean slope -3.0 d yr^{-1}) and end (open circles, mean slope -0.3 d yr^{-1}) of the high-productivity (NPP $\geq$0.5 gC m^{-2} d^{-1}) period in northern Barents Sea.

assume no photosynthesis in the polar night (poleward of the polar circle at approximately 65.5° N), the region of missing data starts already poleward of about 50°. The area of missing ocean colour data in open water reaches over 11 million km^2 every winter in the Northern Hemisphere and is slightly increasing owing to decreasing ice cover. NPP for pixels that had valid PAR but no ice and no ocean colour data after interpolation and extrapolation was calculated assuming a low Chla value (0.1 mg m^{-3}) with estimated PAR. While the total area of this gap filling was large, the effect on total NPP was relatively small owing to the low PAR.

(a) Interannual time series of net primary production in the Arctic Ocean

The monthly maximum in total integrated pan-Arctic NPP (figure 1*b*) has increased approximately 47% from the first half of the time series (1998–2006) to the second half of the series (2007–2015) and is currently estimated at approximately 0.15 PgC month^{-1}. NPP increased sharply from 2006 to 2007, and interannual changes both before and after that were much smaller. In contrast to the increasing NPP, the productivity per open water area (figure 1*c*) has declined by 12.9% from 1998–2006 to 2007–2015, particularly in the period 2009–2010. The annual pan-Arctic NPP (figure 1*d*) has increased more smoothly but the increase is also almost 47%. It appears that both the summer maximum and the annual total reached a plateau in 2011–2012. These changes in NPP are inversely correlated with the extent of sea ice and positively with the open water area. Years with large positive open water anomaly, e.g. 2007 and 2012 (figure 1*e*), have also large positive anomalies in NPP.

Monthly NPP anomalies (calculated by subtracting the climatological monthly mean from the value of the current month) are positively correlated with anomalies in open water area (figure 2*a*,*b*) during the summer months with the strength of

the correlation being highest in July. The effectiveness of open water to generate additional NPP (i.e. the slope of the regression between open water anomaly and NPP anomaly) is highest in June, followed by July and May.

The areas where interannual changes in ice concentration and NPP have occurred are different from month to month. In June (figure 2*c*), the decrease in ice concentration has occurred primarily in the northeastern Barents Sea and between Greenland and the North American continent. There is a good correspondence between areas of June decrease in ice concentration and the increase in NPP, but the area of increased NPP seems to be larger, as if the effects of decreased ice have 'spilled over' to a larger area. In July and August, the areas of increasing NPP move gradually to the east (to the Kara and Laptev seas) and the correspondence between the decrease in ice and increase in NPP becomes low. In August (figure 2*d*), the decrease in ice concentration has occurred primarily off Siberia and in the Beaufort and Chukchi seas, whereas major increases in NPP occurred primarily in different areas (e.g. Barents and Laptev seas).

Owing to earlier ice retreat and later freeze-up (figure 2*e*), the duration of the ice-free period has increased in many areas, e.g. in the Barents Sea. In the northern Barents Sea, the mean trend towards earlier ice retreat has been at a rate of -4.6 ± 0.6 d yr^{-1} and the freeze-up has become later at a mean rate of 1.4 ± 0.3 d y^{-1}. As a result, the ice-free period there has increased 3.5-fold, from approximately 80 days in 1979 to approximately 289 days in 2015 (standard error of the estimate is 40 days). In the same area, the start of the productive period with high NPP (greater than or equal to 0.5 gC m^{-2} d^{-1}) has advanced at a mean rate of -3.0 ± 0.6 d y^{-1} (figure 2*f*) but, in contrast to the later formation of ice, the timing of the end of the high-productive period has not changed significantly. This can be explained by the fact that after the end of the spring bloom, primary production is limited by nutrients and the apparent decrease in satellite-detected NPP may be accentuated by the sinking of the Chla maximum. Still, the length of time between the start and end of the high-productivity period has increased from approximately 15 days in 1998 to 62 days in 2015 (standard error of the estimate is 13 days). For the whole Artic Ocean between latitudes 66°N and 84° N, the mean start of the high-productivity (greater than or equal to 0.4 gC m^{-2} d^{-1}) season has advanced at a mean rate of -0.4 ± 0.1 d yr^{-1}, and the end is delayed at a mean rate of 0.6 ± 0.1 d yr^{-1}. The delay may be related to the appearance of autumn blooms in some areas [18].

3. Conclusion

— The summer monthly maximum and the annual pan-Arctic NPP have increased by 47% from the first half of the time series (1998–2006) to the second half of the series (2007–2015) but changes after 2011 have been minor. The specific productivity per open water area has decreased by 12.9% from the first half to the second half of the series.

— The monthly anomalies in NPP are positively correlated with the summer anomalies in open water area: open water area in June has the strongest effect on increasing NPP, followed by July and May.

— The areas of interannual increase in NPP correspond well to the areas of decreased ice concentration in June, but the correspondence is weak in July and August.

— The high-productivity period starts earlier and extends longer when averaged over the whole Arctic Ocean. In an area of the most dramatic change, the northern Barents Sea, sea ice has been retreating earlier at a mean rate of -4.5 d yr^{-1} and freeze-up is later at 1.4 d yr^{-1}. The high-productivity season is also starting earlier at a mean rate of -3.0 d yr^{-1} but the termination is not becoming later.

Ethics. Analyses did not directly involve animal subjects.

Data accessibility. Datasets of 5 day NPP used in this analysis are available in HDF4 format from the Dryad Digital Repository (http://dx.doi.org/10.5061/dryad.34f4q) [17].

Authors' contributions. M.K. created the time series, performed the analysis and wrote the manuscript. Z.L., C.D.N and B.G.M conceived the study, contributed to interpreting results, critically edited the manuscript, gave final approval of the version to be published and agree to be held accountable for its content.

Competing interests. We declare we have no competing interests.

Funding. Financial support was provided by NASA grants NNX14AL80G, NNX14AM15G and by Hanse-Wissenschaftskolleg to M.K.

Acknowledgement. We thank NASA Ocean Color Processing Group, PO-DAAC, ESA OC-CCI group, NOAA NCDC, National Snow and Ice Data Center Distributed Active Archive Center and CM SAF for satellite data.

References

1. Arrigo KR, van Dijken G, Pabi S. 2008 Impact of a shrinking Arctic ice cover on marine primary production. *Geophys. Res. Lett.* **35**, L19603. (doi:10.1029/2008GL035028)
2. Arrigo KR, van Dijken GL. 2011 Secular trends in Arctic Ocean net primary production. *J. Geophys. Res.* **116**, C09011. (doi:10.1029/2011JC007151)
3. Babin M, Bélanger S, Ellingsen I, Forest A, Le Fouest V, Lacour T, Ardyna M, Slagstad D. 2015 Estimation of primary production in the Arctic Ocean using ocean colour remote sensing and coupled physical–biological models: strengths, limitations and how they compare. *Prog. Oceanogr.* **139**, 197–220. (doi:10.1016/j.pocean.2015.08.008)
4. Bélanger S, Babin M, Larouche P. 2008 An empirical ocean color algorithm for estimating the contribution of chromophoric dissolved organic matter to total light absorption in optically complex waters. *J. Geophys. Res.* **113**, C04027. (doi:10.1029/2007JC004436)
5. Kahru M, Brotas V, Manzano-Sarabia M, Mitchell BG. 2010 Are phytoplankton blooms occurring earlier in the Arctic? *Glob. Change Biol.* **115**, 1733–1739. (doi:10.1111/j.1365-2486.2010.02312.x)
6. Lee ZP, Carder KL, Arnone RA. 2002 Deriving inherent optical properties from water color: a multiband quasi-analytical algorithm for optically deep waters. *Appl. Opt.* **41**, 5755–5772. (doi:10.1364/AO.41.005755)
7. Lee ZP, Darecki M, Carder KL, Davis CO, Stramski D, Rhea WJ. 2005 Diffuse attenuation coefficient of downwelling irradiance: an evaluation of remote sensing methods. *J. Geophys. Res.* **110**, C02017. (doi:10.1029/2004JC002573)
8. Behrenfeld MJ, Falkowski PG. 1997 Photosynthetic rates derived from satellite based chlorophyll concentration. *Limnol. Oceanogr.* **42**, 1–20. (doi:10.4319/lo.1997.42.1.0001)
9. Kahru M, Kudela R, Manzano-Sarabia M, Mitchell BG. 2009 Trends in primary production in the California Current detected with satellite data. *J. Geophys. Res.* **114**, C02004. (doi:10.1029/2008JC004979)
10. Lee YJ *et al.* 2015 An assessment of phytoplankton primary productivity in the Arctic Ocean from satellite ocean color/*in situ* chlorophyll-*a* based models. *J. Geophys. Res. Oceans* **120**, 6508–6541. (doi:10.1002/2015JC011018)

11. Bricaud A, Babin M, Morel A, Claustre H. 1995 Variability in the chlorophyll-specific absorption coefficients of natural phytoplankton: analysis and parameterization. *J. Geophys. Res*. **100**, 13 321–13 332. (doi:10.1029/95JC00463)
12. Frouin R, Franz BA, Werdell PJ. 2003 The SeaWiFS PAR product. In *Algorithm updates for the fourth SeaWiFS data reprocessing* (eds SB Hooker, ER Firestone), NASA Tech. Memo-2003-206892, vol. 22.
13. Lee ZP, Weidemann A, Kindle J, Arnone R, Carder KL, Davis C. 2007 Euphotic zone depth: its derivation and implication to ocean-color remote sensing. *J. Geophys. Res*. **112**, C03009. (doi:03010.01029/02006JC003802)
14. Reynolds RW, Smith TM, Liu C, Chelton DB, Casey KS, Schlax MG. 2007 Daily high-resolution-blended analyses for sea surface temperature. *J. Clim.* **20**, 5473–5496. (doi:10.1175/2007JCLI1824.1)
15. Müller R, Pfeifroth U, Träger-Chatterjee C, Cremer R, Trentmann J, Hollmann R. 2015 *Surface solar radiation data set–Heliosat* (*SARAH*), *satellite application facility on climate monitoring*. Darmstadt, Germany: EUMETSAT. http://dx.doi.org/10.5676/EUM_SAF_CM/SARAH/V001.
16. Cavalieri DJ, Parkinson CL, Gloersen P, Zwally H. 1996 *Sea ice concentrations from Nimbus-7 SMMR and DMSP SSM/I-SSMIS passive microwave data*. Boulder, CO: NASA National Snow and Ice Data Center Distributed Active Archive Center.
17. Kahru M, Lee Z, Mitchell BG, Nevison CD. 2016 Effects of sea ice cover on satellite-detected primary production in the Arctic Ocean. Dryad Digital Repository. (doi:10.5061/dryad.34f4q)
18. Ardyna M, Babin M, Gosselin M, Devred E, Rainville L, Tremblay J-É. 2014 Recent Arctic Ocean sea ice loss triggers novel fall phytoplankton blooms. *Geophys. Res. Lett*. **41**, 6207–6212. (doi:10.1002/2014GL061047)